Highly polarized light emission by isotropic quantum dots integrated with magnetically aligned segmented nanowires

Can Uran, Talha Erdem, Burak Guzelturk, Nihan Kosku Perkgöz, Shinae Jun, Eunjoo Jang, and Hilmi Volkan Demir

Citation: Applied Physics Letters **105**, 141116 (2014); doi: 10.1063/1.4897971
View online: http://dx.doi.org/10.1063/1.4897971
View Table of Contents: http://scitation.aip.org/content/aip/journal/apl/105/14?ver=pdfcov
Published by the AIP Publishing

Highly polarized light emission by isotropic quantum dots integrated with magnetically aligned segmented nanowires

Can Uran,[1] Talha Erdem,[1] Burak Guzelturk,[1] Nihan Kosku Perkgöz,[1,2] Shinae Jun,[3] Eunjoo Jang,[3] and Hilmi Volkan Demir[1,4,a)]

[1]*Department of Electrical and Electronics Engineering, Department of Physics, and UNAM - National Nanotechnology Research Center, Institute of Materials Science and Nanotechnology, Bilkent University, Ankara 06800, Turkey*

[2]*Department of Electrical and Electronics Engineering, Faculty of Engineering, Anadolu University, Eskisehir 26555, Turkey*

[3]*Inorganic Material Laboratory, Material Research Center, Samsung Advanced Institute of Technology, Samsung Electronics Co., 130 Samsung-ro, Yeongtong-gu, Suwon-si, Gyeonggi-do 443-803, South Korea*

[4]*Luminous! Center of Excellence for Semiconductor Lighting and Displays, School of Electrical and Electronic Engineering, School of Physical and Materials Sciences, Nanyang Technological University, Singapore, Singapore 639798*

(Received 29 August 2014; accepted 4 September 2014; published online 10 October 2014)

In this work, we demonstrate a proof-of-concept system for generating highly polarized light from colloidal quantum dots (QDs) coupled with magnetically aligned segmented Au/Ni/Au nanowires (NWs). Optical characterizations reveal that the optimized QD-NW coupled structures emit highly polarized light with an s-to p-polarization (s/p) contrast as high as 15:1 corresponding to a degree of polarization of 0.88. These experimental results are supported by the finite-difference time-domain simulations, which demonstrate the interplay between the inter-NW distance and the degree of polarization. © *2014 AIP Publishing LLC*. [http://dx.doi.org/10.1063/1.4897971]

Linear optical polarizers are passive components that selectively transmit the light with electric field parallel to the transmission axis (s-polarization) and block the transmission of the electromagnetic field in the orthogonal polarization (p-polarization). Polarizers are crucial for various optical systems and extensively used in applications ranging from imaging[1] and liquid crystal displays (LCDs).[2] In the case of LCDs, an unpolarized light generated in the backlight unit is converted into a polarized light via a polarizer. This polarization process contributes to the most significant loss in the LCDs. Thus, achieving polarized light-emitting sources are highly welcomed, which are expected to increase the optical efficiency of the LCDs. To date, various polarizing optical media were integrated with light-emitting materials to achieve polarized light sources. Wire-grid based polarizer,[3] resonant cavity,[4] plasmonic nanocavity,[5] birefringent crystal,[6] and liquid crystal integrated fluorescent materials[7] can be employed to realize polarized light emission. Wire-grid polarizers have shown very good performance in terms of the degree of emission polarization. Zhang *et al*. reached the vertical (s) to parallel (p) polarization contrast of 7:1 using metallic nanogratings fabricated by electron beam lithography on top of a conventional InGaN/GaN LED.[8] Ma *et al*. obtained an s/p polarization contrast as high as 50:1, corresponding to a polarization degree of about 0.96.[9] However, such approaches require special nanolithography techniques to achieve polarized light in the visible spectrum.[3] Sub-wavelength parallel metallic features are usually fabricated using techniques including focused ion beam lithography,[10] electron beam lithography,[11] and nanoimprint lithography.[12,13] Nevertheless, these techniques are expensive, time consuming, and low throughput. Alternatively, deposition of metal nanoparticles via layer-by-layer assembly was employed to realize polarized emission via utilizing the plasmonic nanocavity effect by Ozel *et al*.[5] In these multilayered plasmonic nanocavities polarized light emission with s/p polarization degree of 0.80 was observed.

As an alternative approach, here, we show highly polarized light emission in coupled thin films of colloidal quantum dots (QDs) and magnetically aligned multi-segmented nanowires (NWs). These NWs consist of ferromagnetic (Ni) parts that enable alignment under externally applied magnetic field. In-template synthesis of these NWs together with their magnetic field assisted alignment facilitates the fabrication of massive number of highly parallel NWs over large area thin films with low cost and fast production technique. Previously, various alignment techniques have been employed including Langmuir-Blodgett,[14] external electric assisted alignment[15,16] and as well as those based on magnetic field assisted alignment.[17,18] Among these techniques, some may require a more complex alignment setup as in the case of Langmuir-Blodgett assembly or pre-defined electrodes as in the case of electric field assisted assembly. Among these, magnetic field assisted assembly using centimeter sized commercially available magnets is a versatile tool to align NWs having ferromagnetic parts on surfaces or NWs inside a host medium without the requirement for a pre-defined electrode or surface functionalization. This makes magnetic field assisted alignment a promising candidate for making polarizing structures.

As a proof-of-concept demonstration, here, we demonstrate highly polarized emission using the isotropic emitter CdTe QDs by integrating them with the aligned three-segment Au/Ni/Au NWs. The NWs were plated using template-assisted electrodeposition method,[16,19] and aqueous CdTe QDs were synthesized colloidally as described in

a)Electronic mail: volkan@stanfordalumni.org. Tel.: +90 (312) 290-1021. Fax: +90 (312) 290-1123.

Ref. 20. QDs represent an important class of emitters, which are highly suitable as white-light engines for backlight of the LCDs owing to their spectrally pure color emission that can be easily matched to the color filters of LCDs to boost the optical performance. The resulting hybrid system exhibited polarized emission in visible spectrum with an s/p polarization contrast as high as 15:1 corresponding to a polarization degree of 0.88.

The details of the synthesis of the aqueous CdTe QDs are given in supplementary material. Fig. S1 shows the absorption and emission spectra of the synthesized CdTe QDs.[21] Using the Whatman Anodisc membrane (with a pore density of $10^9\,cm^{-2}$) as our template, three-segment Au/Ni/Au NWs having diameters of ca. 250 nm were plated by employing electrodeposition method. Prior to the plating, a 200 nm thick silver layer serving as the working electrode was thermally evaporated on the backside of the membrane. As the counter electrode mesh platinum was used that was placed 5 cm above the membrane inside an O-ring glass tube. The process started with the electrodeposition of 2 μm thick silver using the silver bath (TechniSilver E-2, Italgalvano, 11.5% potassium silver cyanide) to clog the branching portion of the membrane. For gold segments, we used Orotemp 24 (6.87% potassium aurocyanide) and drove -1.6 mA current by Versastat 3 potentiostat to deposit approximately 1.5 μm long Au segments. After rinsing, we drove -1.6 mA current again to deposit nickel using the nickel bath, which is composed of nickel sulfamate (20%–35%), nickel bromide (0.5%–1.5%), and boric acid (1%–3%), to obtain 7 μm long nickel segments. The final gold segments of $\sim$1.5 μm in length were plated as in the first step following the rinsing. At these current levels, the average deposition rates of gold and nickel were 2 and 1.5 nm/s, respectively. Gold segments constituted of ca. 3 μm and the remaining $\sim$7 μm of the NWs was nickel (Figs. 1(a) and 1(b)). After deposition, the silver back-coating was etched with a nitric acid solution (HNO_3 of 30%) and the alumina disc was dissolved in a sodium hydroxide solution (NaOH of 3M). The synthesized NWs remained in the base solution. Finally, the NWs were centrifuged three times in DI water at 3000 rpm and stored in DI water.

An externally applied magnetic field enables magnetization of these NWs and helps to rotate and position them along the direction of the applied field. This is mainly due to their high aspect ratio geometry, which allows the Ni parts of the NWs to experience higher magnetization and induce magnetic charges to interact with the external magnetic field. As a result, a torque is exerted on the NWs causing them to align in the direction of the field. The induced magnetic moment (L) can be expressed using the relation $L = mlH \sin\theta$, where m, l, H, and θ denote the induced dipole strength, the ferromagnetic segment length, the external magnetic field, and the angle between the magnetic field and the longitudinal axis of the NW, respectively.[17] Longer the ferromagnetic segment length (l) of the NWs and/or higher the external magnetic field (H), we observe a higher torque induced on the wires, thus leading to a better alignment. The aligned metal NWs constructed a grid-like architecture in which they act as a good reflector for one polarization while they transmit a higher portion of the electromagnetic field with the perpendicular polarization.

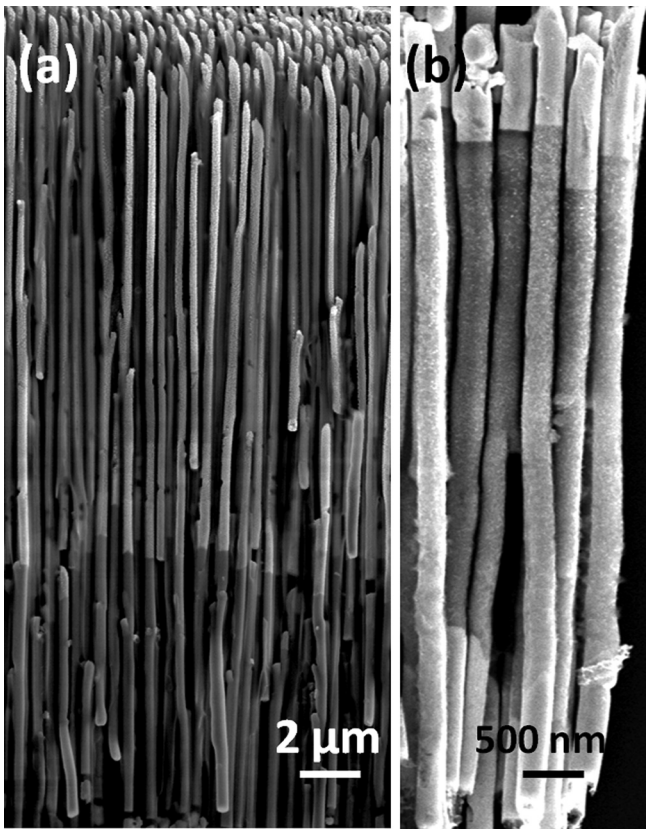

FIG. 1. Arrays of Au-Ni-Au segmented NWs (a) inside the alumina membrane and (b) the NWs immobilized on glass after etching of the membrane.

To investigate the potential of the assemblies of these segmented NW to achieve polarized light from the QDs, we numerically investigated the hybrid architecture comprising of aligned metal NWs and CdTe QDs using finite difference time domain (FDTD) technique (Fig. 2). Single segment NWs comprising of 10 μm long Ni were used in the simulations in addition to Au-Ni-Au three segment NWs having 1.5 μm long Au segments and 7 μm long Ni segment to understand the effects of Au segments in the polarizing effect of the obtained emission. The QD layer is modeled using the real and imaginary parts of the refractive index as measured by optical ellipsometry. In the FDTD simulations, light emitted by the QD film is assumed to pass through the aligned NW network, each of which are randomly positioned NWs having average NW-to-NW separation of 250, 300, 350, and 400 nm. This randomly distributed NW matrix is along the lateral plane to account for the very large area of the sample that can be up to a few cm^2. We separately investigated the parallel and perpendicular polarization that is emitted by the QDs and monitored the transmitted power for these two orthogonal polarizations.

Along the longitude of the NWs, parallel polarized electric field components of the emitted light experiences a conductive medium and is absorbed/scattered. On the other hand, perpendicular polarized electric field components of the emitted light interact much less with the aligned NWs; thus, perpendicular polarized light is transmitted more. The results of the simulations were presented in Figs. 2(a) and 2(b). According to these results, aligned Au/Ni/Au and Ni NWs exhibit anisotropic character (i.e., increasing s/p

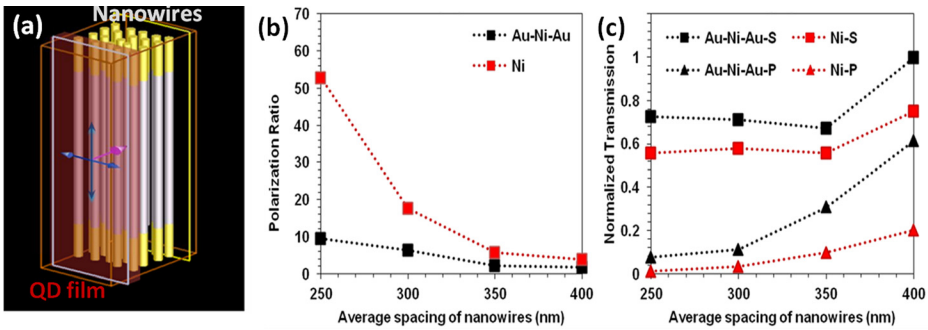

FIG. 2. (a) A representative image illustrating FDTD simulation structure. (b) Numerical simulation results indicating the ratio of s- and p-polarizations transmitted through Au/Ni/Au and Ni NWs at the emission peak of QDs (~650 nm). (c) Normalized transmitted intensities through Au/Ni/Au and Ni NWs at the emission peaks of QDs for s- and p- polarizations.

polarization contrast for the transmission) that is enhanced as the inter-NW distance is decreased. In the case of Au/Ni/Au NWs, polarization contrast larger than 10:1 is possible to achieve with inter-NW distance that is smaller than 250 nm. In the case of Ni NWs, higher polarization contrast could be achieved at the expense of reduced transmitted power since Ni introduces extra loss due to the absorption.

For the magnetic alignment, two neodium magnets, each of 5 mm × 10 mm × 40 mm in size and generating a magnetic field of 400 Gauss, were used to align the NWs. For a proof-of-concept demonstration, Au/Ni/Au NWs were used instead of Ni NWs, which tend to break during the etching process of the silver from the back of the membranes. In addition, post thermal baking process strengthens the Au/Ni interface to keep segmented NWs robust and undamaged. To avoid quenching of the emission of the QDs and obtain an appropriate level of viscosity so that the NWs were not pulled to the sides of the film while drying, poly(vinyl pyrolidone) (PVP) was used as a host material. We prepared two different films comprising of the same amount of QDs but having different amounts of NWs. 500 μL of the multi-segmented NW in water was mixed with 750 μL of PVP, and 1600 μL CdTe QD solution was mixed with 1200 μL of PVP. The NW:PVP solutions (375 and 500 μL) were drop-casted on a glass substrate and left for drying overnight under magnetic field. Since PVP provides a reasonable viscosity, it allows controlling the positioning of NWs as it is required for a higher polarization contrast. Furthermore, once it dries, PVP is a strong host material to keep the NWs in the orientation that they were aligned and provide a three dimensional structure where the NWs are highly aligned along one dimension. Subsequent to the deposition of the NWs, QD:PVP solution (700 μL) was drop-casted over the NW films and again the system was left for drying overnight. The hybrid film architecture and the alignment setup are illustrated in Fig. 3(a).

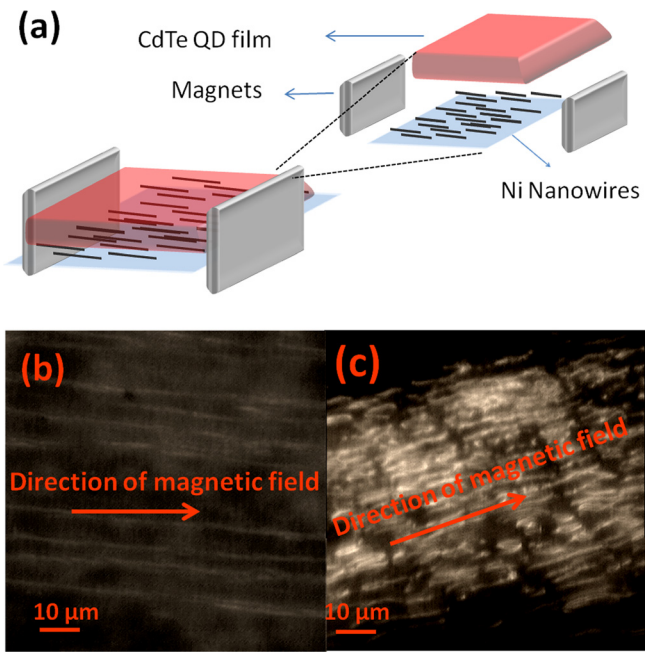

FIG. 3. (a) Alignment during hybridization the CdTe QDs with aligned ferromagnetic NWs in PVP host film between two Neodium magnets. Microscopy images of (b) uniformly distributed NWs, and (c) dense and uniformly distributed NWs.

As the optical microscopy images show, the NWs were clearly aligned in the direction of the magnetic field and form a one dimensional array. The uniform alignment regions, where the NWs tend to form regular grid like structures are shown in Figs. 3(b) and 3(c). Due to the random nature of the alignment process, non-uniformities cannot be completely avoided, which would limit the extinction ratio (the ratio of the s-polarized light to p-polarized light). However, still reasonably large values were obtained depending on the amount of the NWs as explained in the characterization section.

Our optical characterization setup is illustrated in Fig. 4. These QD integrated NW hybrid films were excited using a laser diode emitting at 375 nm. The emitted light by the QDs was collected through a linear polarizer, monochromator and a photomultiplier tube. The emission intensity of the QDs was recorded as the polarizer is rotated to measure the perpendicular and parallel polarization components of the light emitted by the QDs that is transmitted through the NWs.

When bare CdTe QDs were employed, which were not integrated to the NWs, unpolarized light is emanated at peak emission wavelength of ~650 nm in solid-film. The s/p polarization contrast is close to 1:1. When the QDs are

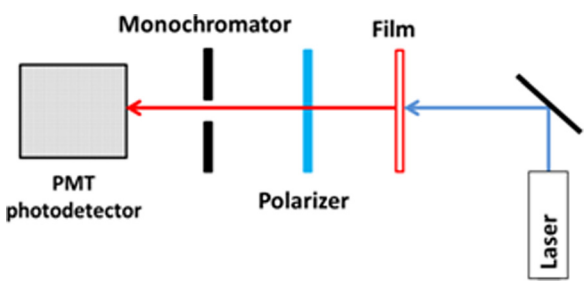

FIG. 4. Illustration of the characterization setup for the polarization degree of the QD integrated aligned NW films.

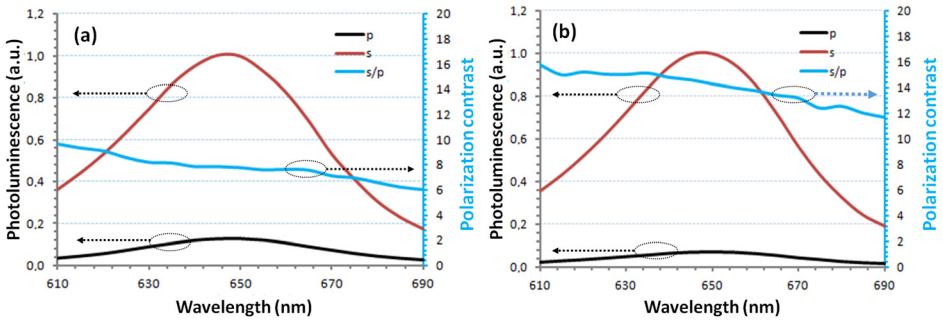

FIG. 5. Photoluminescence spectra intensity of the QDs integrated on the NW:PVP samples in s- and p- polarizations (red and black lines) along with the s/p contrast (blue line) from (a) the thinner and (b) the thicker NW:PVP film. The maximum contrast of the polarizations was found to be 10:1 for the thinner film and 15:1 for the thicker one.

decorated on top two different NW films having different thickness (375 and 500 μl of NW:PVP). The emission intensities of the QDs collected by detector after the emission side polarizer in s- and p-polarizations are presented in Fig. 5 for the thin and thick NW matrices. The blue curves in Fig. 5 show the s/p polarization contrast as a function of the wavelength. Our results reveal that aligned NWs in PVP matrix substantially polarizes the emission of the QDs. For the thin NW:PVP sample, s/p polarization contrast is up to 10:1, while it is up to 15:1 for the thicker NW:PVP sample. We attribute this to the increased number of aligned NWs that enhances the polarization contrast. We further observe that the contrast of the polarizations has a slowly varying trend with respect to the wavelength. We attribute such a large bandwidth of the polarization contrast due to the random nature of the hybrid films, where the distribution of the aligned NWs is not uniform within the film.

In summary, we proposed and demonstrated a proof-of-concept hybrid thin film system for the generation of polarized light with a polarization contrast of perpendicular to parallel polarizations larger than 15:1 in the visible range by employing multi-segmented NWs having ferromagnetic parts, which are well aligned under external magnetic field. The proposed approach makes use of a much cheaper and easier fabrication procedure compared to the conventional expensive fabrication techniques. Furthermore, we verified the experimental results of highly polarized light generation by FDTD simulations, which revealed the relation between inter-NW distance and the achieved polarization contrast.

This work was supported by Samsung Global Research Outreach (GRO) program, ESF EURYI, EU-FP7 Nanophotonics4Energy NoE, and TUBITAK EEEAG 107E088, 109E002, 109E004, 110E010, 110E217, 111E189, and 112E183. T.E. acknowledges TUBITAK-BIDEB for the financial support. N.K.P. particularly acknowledges the support from Anadolu University (BAP-1306F174).

[1]R. Oldenbourg, Nature **381**, 811 (1996).
[2]C. Weder, C. Sarwa, A. Montali, C. Bastiaansen, and P. Smith, Science **279**, 835 (1998).
[3]Z. Yu, P. Deshpande, W. Wu, J. Wang, and S. Y. Chou, Appl. Phys. Lett. **77**(7), 927 (2000).
[4]S. Saraf, R. L. Bayer, and P. J. King, Appl. Opt. **46**, 3850 (2007).
[5]T. Ozel, S. Nizamoglu, M. A. Sefunc, O. Samarskaya, I. O. Ozel, E. Mutlugun, V. Lesnyak, N. Gaponik, A. Eychmüller, and S. V. Gaponenko, ACS Nano **5**, 1328 (2011).
[6]S.-T. Wu, U. Efron, and L. D. Hess, Appl. Opt. **23**, 3911 (1984).
[7]A. Szabo, J. Chem. Phys. **72**, 4620 (1980).
[8]L. Zhang, J. H. Teng, S. J. Chua, and E. A. Fitzgerald, Appl. Phys. Lett. **95**, 261110 (2009).
[9]M. Ma, D. S. Meyaard, Q. Shan, J. Cho, E. F. Schubert, G. B. Kim, M.-H. Kim, and C. Sone, Appl. Phys. Lett. **101**, 061103 (2012).
[10]J. Feng, Y. Zhao, X.-W. Lin, W. Hu, F. Xu, and Y.-Q. Lu, Sensors **11**, 2488 (2011).
[11]B. Schnabel, E.-B. Kley, and F. Wyrowski, Opt. Eng. **38** (2), 220 (1999).
[12]J. J. Wang, L. Chen, X. Liu, P. Sciortino, F. Liu, F. Walters, and X. Deng, Appl. Phys. Lett. **89**, 141105 (2006).
[13]J. J. Wang, J. Deng, X. Deng, F. Liu, P. Sciortino, L. Chen, A. Nikolov, and A. Graham, IEEE J. Sel. Top. Quant. Electron **11**, 241 (2005).
[14]D. Whang, S. Jin, Y. Wu, and C. M. Lieber, Nano Lett. **3**(9), 1255 (2003).
[15]J. Boote and S. Evans, Nanotechnology **16**, 1500 (2005).
[16]C. Uran, E. Unal, R. Kizil, and H. V. Demir, IEEE J. Sel. Top. Quant. Electron **15**, 1413 (2009).
[17]C. M. Hangarter, Y. Rheem, B. Yoo, E.-H. Yang, and N. V. Myung, Nanotechnology **18**, 205305 (2007).
[18]M. G. Bellino, E. J. Calvo, and G. J. Gordillo, Phys. Status Solidi RRL **3**, 1 (2009).
[19]S. Liu, J. B.-H. Tok, and Z. Bao, Nano Lett. **5**, 1071 (2005).
[20]M. Grabolle, M. Spieles, V. Lesnyak, N. Gaponik, A. Eychmüller, and U. Resch-Genger, Anal. Chem. **81**, 6285 (2009).
[21]See supplementary material at http://dx.doi.org/10.1063/1.4897971 for details of CdTe quantum dot synthesis, and their absorption and emission spectra.